J. Fluid Mech. (2006), *vol.* 549, *pp.* 385–402.
doi:10.1017/S0022112005007925 Printed in the United Kingdom

Passive propulsion in vortex wakes

By D. N. BEAL[1], F. S. HOVER[1], M. S. TRIANTAFYLLOU[1], J. C. LIAO[2] AND G. V. LAUDER[2]

[1]Department of Ocean Engineering, Massachusetts Institute of Technology, Cambridge, MA, USA

[2]Department of Comparative Zoology, Harvard University, Cambridge, MA, USA

(Received 30 August 2004 and in revised form 1 August 2005)

A dead fish is propelled upstream when its flexible body resonates with oncoming vortices formed in the wake of a bluff cylinder, despite being well outside the suction region of the cylinder. Within this passive propulsion mode, the body of the fish extracts sufficient energy from the oncoming vortices to develop thrust to overcome its own drag. In a similar turbulent wake and at roughly the same distance behind a bluff cylinder, a passively mounted high-aspect-ratio foil is also shown to propel itself upstream employing a similar flow energy extraction mechanism. In this case, mechanical energy is extracted from the flow at the same time that thrust is produced. These results prove experimentally that, under proper conditions, a body can follow at a distance or even catch up to another upstream body without expending any energy of its own. This observation is also significant in the development of low-drag energy harvesting devices, and in the energetics of fish dwelling in flowing water and swimming behind wake-forming obstacles.

1. Introduction

Fish commonly reside in high-energy environments such as rivers, streams and coastal surf zones. It seems reasonable that fish may adopt behaviours to reduce energy expenditure, and indeed, salmon and trout have been found to entrain behind obstacles to optimize their net energy expense (Fausch 1984), a function of local currents and the availability of food. The lateral line, an array of mechanosensory cells distributed along the body of most fish, potentially enables them to detect pressure discontinuities so as to select favourable hydrodynamic conditions in the flow (Sutterlin & Waddy 1975; Braun & Coombs 2000).

The simplest representative situation is to consider a fish in the wake of a bluff cylinder. Under highly idealized conditions, a wake can be viewed as a body of water that is stationary with respect to the bluff body, confined within two thin shear layers emanating from the body. Under such idealized conditions, a fish could stay stationary, requiring no energy input, or even swim slowly upstream, requiring very small but positive energy. Reality is quite different, however, since a strong instability and mixing of the shear layers develops at Reynolds numbers higher than $Re = 50$, resulting in the formation of the Kármán street. At a short distance downstream, typically beyond two body diameters, the wake develops a net downstream average velocity component, marking the end of the so-called suction region; hence, beyond two diameters downstream, the time-average wake causes a net drag on a fish. This drag force increases with distance downstream from the bluff body, eventually reaching the drag value for open flow. Hence, a fish would be expected to require positive mechanical energy to overcome the average drag force in order to follow the

bluff body, at any distance beyond about two diameters. In an unsteady wake, a fish could take advantage of the unsteady flow by strategic path-planning through the vortex wake so as minimize the oncoming flow speed, and hence drag, at any given time. However, beyond two diameters downstream from the cylinder, the vortices are not strong enough to reverse the flow, i.e. to direct it upstream, hence the fish must still work against drag, even though that drag is smaller than in open flow.

In the present work, we show that the conclusions above, which are based on time-averaged flow considerations, are not applicable, and, instead, that fish can swim upstream without any energy of their own; they extract the required energy from the oncoming large-scale vortices. We describe a set of experiments performed with rainbow trout (*Oncorhynchus mykiss*) within a flow channel containing a vertically mounted cylinder. Being a lotic (stream-dwelling) fish, rainbow trout are expected to have evolved shape and function in such a way as to take advantage of the obstacles presented to them, that is, in order to minimize their energy consumption. In fact, previous experiments, described by Liao *et al.* (2003*a*, *b*), showed that live trout do alter their swimming motions to synchronize with the incoming wake shed by an upstream cylinder in both frequency and phase, implying that the trout are using the vorticity for energy benefit. Here, we demonstrate that a dead fish may first synchronize with a vortex wake, and then move forward against the flow, well outside the suction region. This proves that trout are, in fact, capable of recovering enough energy from the unsteady wake to use it for propelling themselves.

To extend this conclusion from the dead fish experiments to mechanical devices, and to demonstrate the applicability of these results in an engineering context, we also show that a flexibly mounted two-dimensional rigid foil, through fluid-induced motion only, is capable of producing net thrust using a negative mechanical power input, i.e. all the required mechanical power is extracted from the flow. These experiments place the present results within the context of vorticity control studied with the same apparatus in Gopalkrishnan *et al.* (1994) and Anderson (1996) and are even more notable in terms of the extent of energy extraction since the foil is of very high aspect ratio, with a span equal to that of the cylinder span.

What is novel in both of the present experiments is that a fish or foil can extract sufficient energy from a vortical stream to overcome its own drag, implying that a flapping body can follow another wake-producing body, even at a distance, without expending any energy. This is the principal result of the study.

2. Unsteady mechanisms of energy extraction and thrust production

Energy extraction from an oncoming flow can be achieved in many ways; for example, through a turbine which develops lift in each blade, and hence torque, without the need for external mechanical energy input. Under such steady-state conditions, however, the momentum theorem requires that energy extraction results in the development of a drag force. Hence, the mechanism of combined energy extraction and thrust development must be an unsteady one.

In this regard, Wu (1972) and Wu & Chwang (1974) showed theoretically that a foil heaving and pitching within a wavy stream, produced by travelling water waves, is capable of producing thrust and extracting energy passively. Wu (1972) identified three important regimes, where (i) the wavy stream increased the efficiency of the foil by a combination of increasing thrust and/or decreasing power input; (ii) the foil produced thrust with an efficiency greater than 100 %, recovering energy from the flow, while still requiring a power input to maintain motion; (iii) the foil was capable

of producing thrust and extracting energy in a fluid-excited motion, meaning that no power input from the foil was required.

Wu points out that these results are not limited to water waves: 'It makes little difference to the subsequent discussion if other kinds of wavy streams are considered as long as the transverse velocity of the basic flow can be represented by ... $V_o(x,t) = iA_o e^{i(\omega_o t - kx)}$', (Wu 1972). Wu's linear theory required the assumptions that there is no separation from the leading edge of the foil, that the lateral flow velocities are much smaller than the forward velocities, and that the wavelength of the surface waves is long relative to the foil chord, which are not satisfied in the experimental cases presented in this work. Isshiki & Murakami (1984) experimentally verified Wu's earlier work for the case of harmonic waves in the absence of an oncoming stream, showing that a heaving and pitching foil, passively attached with springs, can produce thrust during fluid-induced motions from surface waves.

In the case of a vortical flow, Koochesfahani & Dimotakis (1988), Gopalkrishnan *et al.* (1994), Streitlien, Triantatyllou & Triantafyllou (1996), Anderson *et al.* (1998) and So, Jadic & Mignolet (1999) have explored the effect of oncoming vorticity, produced by an upstream bluff cylinder, on the foil performance. The basic modes of foil–vortical wake interaction are as follows.

Vortex interception mode. When the leading edge of the foil intercepts the vortices, then thrust is increased and the wake downstream of the foil is altered substantially through strong foil–vortex and cylinder–vortex interactions.

Slaloming mode. The leading edge of the foil approaches, but does not intercept, the oncoming vortices. The wake consists of pairs of vortices, one vortex produced by the foil and one by the cylinder. This mode results in high propulsive efficiency.

In these studies, the foil had high aspect ratio, and the upstream cylinder had dimensions comparable to the dimensions of the foil; as a result, the vortices shed by the foil were of approximately similar strength and aspect ratio to those of the upstream cylinder.

Allen & Smits (2001) have shown that a piezoelectric membrane subject to the action of oncoming vortices from a bluff body can extract energy from the flow. Streitlien *et al.* (1996) have shown theoretically that a foil can extract energy from oncoming vortices resulting in propulsive efficiency higher than 100 %.

Fish employ several unsteady mechanisms to minimize their propulsive exertion. In still water, as the body undulates with a wave passing from the head to tail, body-bound vortices are formed, and pass down the body. The tail, rather than cutting through a uniform incoming flow, interacts with the vorticity produced when this body-bound vorticity is shed into the fluid (Anderson 1996; Mueller *et al.* 1997). Similarly, the tail has been found to interact with vortices shed by the anal and dorsal fins in a beneficial way (Videler 1993; Wolfgang *et al.* 1999; Drucker & Lauder 2001; Mueller *et al.* 2001; Tytell & Lauder 2004). There are cases also in which fin-based swimmers can benefit from interacting with external vorticity. For instance, it has been hypothesized that schooling can serve a hydrodynamic benefit, with fish in the second rank (swimming between the thrust wakes created by those in the first rank) seeing a 40–50 % reduction in incoming velocity (Fish 1999). Dolphins surf in the bow waves of ships (Fejer 1960), and whales gain significant thrust benefits from swimming near surface waves, owing to the oscillating flow over the tail fluke (Bose & Lien 1990). It has been estimated that, if the tail-foil is moving synchronously with the wavy stream, and if the body-length of the whale is not much smaller than the wavelength of the surface waves, a whale could 'absorb up to 25 % of its required propulsive power in head seas and 33 % of propulsive

power in following seas', (Bose & Lien 1990). Anecdotal stories from whalers tell of dead whales coasting at approximately one knot for long periods of time, implying that fluid-excited motion and thrust production can occur for a dead whale in surface waves.

More recently, experiments performed by Liao *et al.* (2003*a*, *b*) demonstrated that rainbow trout placed within a flow channel containing a vertically mounted cylinder would synchronize their swimming frequency with that of the vortex wake, in a high-amplitude high-wavelength motion referred to as the 'Kármán gait'. Experiments using particle image velocimetry (PIV) to visualize the incoming flow field showed that the trout also synchronize the phase of their body oscillations so that the centre-of-mass moves back-and-forth with the external lateral flow (Liao *et al.* 2003*b*). An electromyographic study of the axial muscle described in the same reference illustrates a significant reduction in activity while the trout is entrained behind the cylinder, as opposed to swimming within the free stream.

3. Euthanized trout

In order to test the hypothesis that a fish can passively produce thrust through fluid-induced motion in a Kármán wake, a dead trout was tied to a string attached to a fixed vertical cylinder in a uniform flow; all tests were performed prior to *rigor mortis*.

3.1. *Methods*

Tests were performed at a recirculating tank in the Department of Comparative Zoology, Harvard University. The flow channel's test section was 80 cm long with a 28×28 cm cross-section. A variable-speed pump was used to set the flow velocity in the channel, and the pump speeds were calibrated to flow speed using PIV. A baffle of flow straighteners was placed at the upstream end of the test section in order to reduce the turbulence of the incoming flow.

A high-speed digital video camera (RedLake Motionscope PCI-500) was set up to record the silhouette of the fish within the flow channel at 250 frames per second, with a backlit ventral view, as seen in figure 1. The video was passed through a digitizing program which returns the outlines and mid-lines of the fish at each time step, with a discrete number of body-points along the mid-line (30 in this case). This information was analysed to give the tail-beat frequency, amplitudes and wavelength as discussed in Liao *et al.* (2003*a*); the frequency and wavelength of the trout tail-beats were then compared to the expected values for the cylinder wake.

For our tests, a single trout was killed using MS-222, a general anaesthetic which shuts down nerve cells, both in the brain and the body. In small doses, this effect is temporary, and it is used to anaesthetize fish for surgeries. In large doses, however, its effects are fatal, and a bath of highly concentrated MS-222 for one hour is the standard method for killing fish. The dead fish (length $L_f = 17.8$ cm) was an individual used previously in the EMG experiments (Liao *et al.* 2003*b*).

A line was hooked to the fish and tied to the cylinder, which was held stationary. The cylinder had diameter $D = 5$ cm and a D-shaped cross-section. The line was not significantly compliant and, when taut, held the fish 4 diameters downstream of the cylinder, specifically, in the range in which live fish were seen to hold station. The flow speed was set to 57 cm s^{-1}, or 3.20 L_f s^{-1}, similar to the relative flow speed used in previous tests and resulting in a Reynolds number based on a cylinder diameter of 28 500.

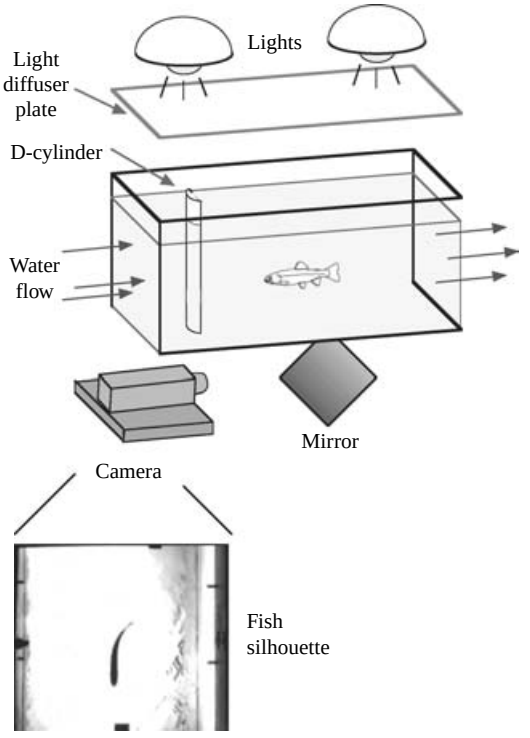

FIGURE 1. The silhouette of the trout was recorded with a high-speed video camera. Flow was measured with PIV in the absence of the trout.

A stationary D-section cylinder in a flow produces a Kármán wake, with stronger vortices than a circular cylinder, with a Strouhal number for vortex shedding, St_c, of approximately 0.2 for this Reynolds-number range (Gopalkrishnan *et al.* 1994). However, in this case the constriction effects from the cylinder in the flow channel were non-negligible, at 18 %. Hence, the expected shedding frequency was adjusted using

$$U_c = U\left(\frac{W}{W-D}\right), \tag{1}$$

$$St_c = \frac{f_c D}{U_c}, \tag{2}$$

where W is the width of the flow channel, U_c is the constricted velocity, and f_c is the shedding frequency, 2.74 Hz in this case. The lateral vortex spacing can be estimated as the cylinder diameter, and the wake wavelength was estimated as $\lambda_w = U/f_c = 20.8$ cm, because although the cylinder shedding would be determined by the constricted flow, the vortices would then be carried downstream by the unconstricted flow. This method for estimating the constricted shedding frequency and the general form and geometry of the wake was verified using PIV in Liao *et al.* (2003*a*).

It was necessary to show that the fish did not begin its forward motion from within the suction region behind the cylinder, usually estimated at $2.0D$ (Gerrard 1966). Hence, the mean and minimum downstream flows at the location of the fish were measured with PIV. Figure 2 shows velocity vectors and vortex arrangement in the wake at a distance of x/D from 2.5 to about 6.5, covering the entire range of interest in these experiments. Although this is an instantaneous velocity field, almost

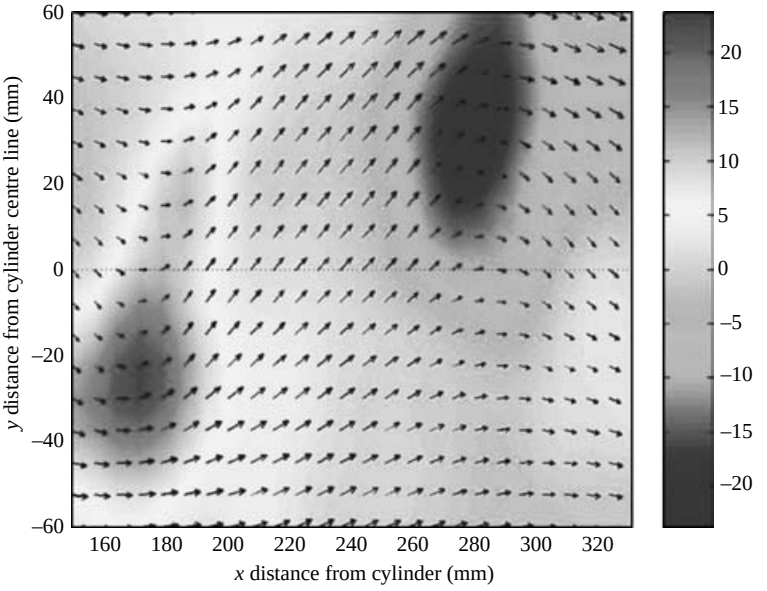

FIGURE 2. Velocity and vorticity field (PIV) covering a distance from 2.5 to about 6.5 diameters downstream from the cylinder (x-axis) and a transverse distance of $\pm 1.2D$.

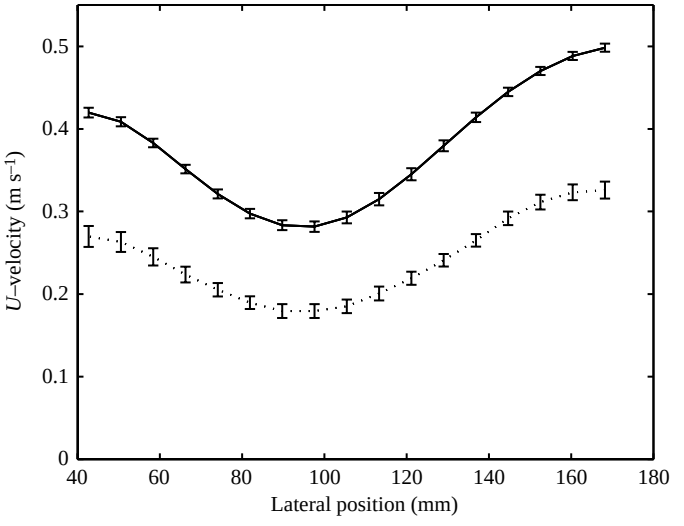

FIGURE 3. The ——, mean and ···, minimum downstream velocities encountered by the fish in its default location 20 cm back from the cylinder. The flow at the two sides does not match perfectly owing to the dorsal mirror in the flow during the PIV tests of Liao *et al.* (2003*b*).

an entire wavelength in the wake is covered, where it is clearly shown that axial flow is everywhere in the downstream direction, while vortices are clearly defined and the wake retains roughly the same features over the entire x/D range shown. This test showed that the fish was not in the suction region, and furthermore, that at no time during the cycle was there even instantaneously an upstream flow near the fish, as also seen in figure 3. We determined that the suction boundary exists at about $1.75D$ downstream of the cylinder.

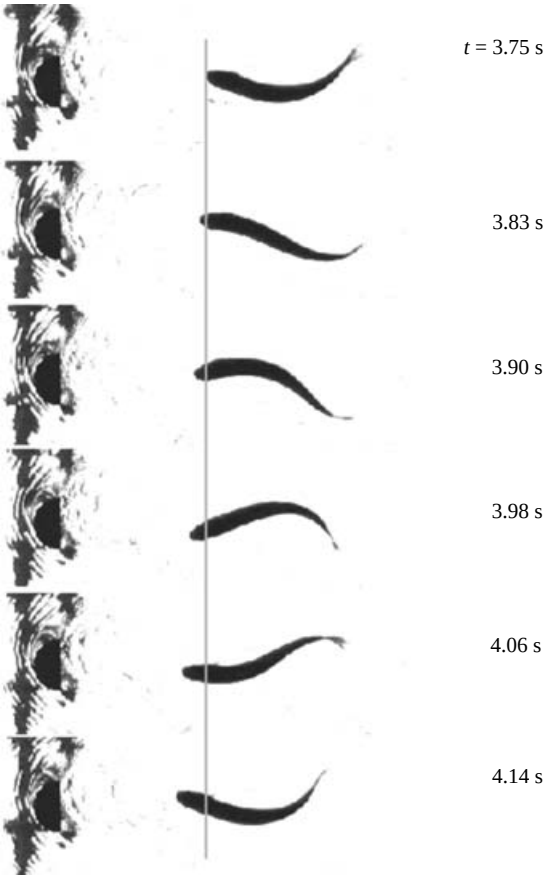

FIGURE 4. The oscillating fluid induces lateral motion on the dead trout's body as well as thrust on the tail, accelerating the body forward against its own drag. The times given correspond to times in figure 4.

Six tail-beats of forward motion were digitized, for which the line is clearly no longer taut, but the fish is still away from the suction region. Every fourth frame of the video was analysed, giving a sample frequency of 62.5 Hz.

3.2. *Results*

When in the Kármán wake, the dead fish repeatedly synchronized with the wake and moved upstream until it entered the suction region behind the cylinder and then ran into the cylinder itself, before tumbling back downstream. The forward motion is illustrated in figure 4. Since PIV showed that both the mean axial velocity and the minimum value of the axial (unsteady) velocity at that location were never negative (i.e. it always pointed downstream), this result implies that the dead fish was moving forward against its own drag owing to energy extraction from the vortex wake.

In order to make certain that the effect was not due to snap of the line (storage of potential energy in the line due to the drag force, and then sudden line-snap and energy release), or some other mechanism pulling the fish forward, the video was digitized and analysed to study the fish kinematics. Figure 5 shows a typical case. Initially, the fish is being buffeted back and forth by the flow, and its frequency of motion does not necessarily match that of the wake. At around 3.7 s, in this particular

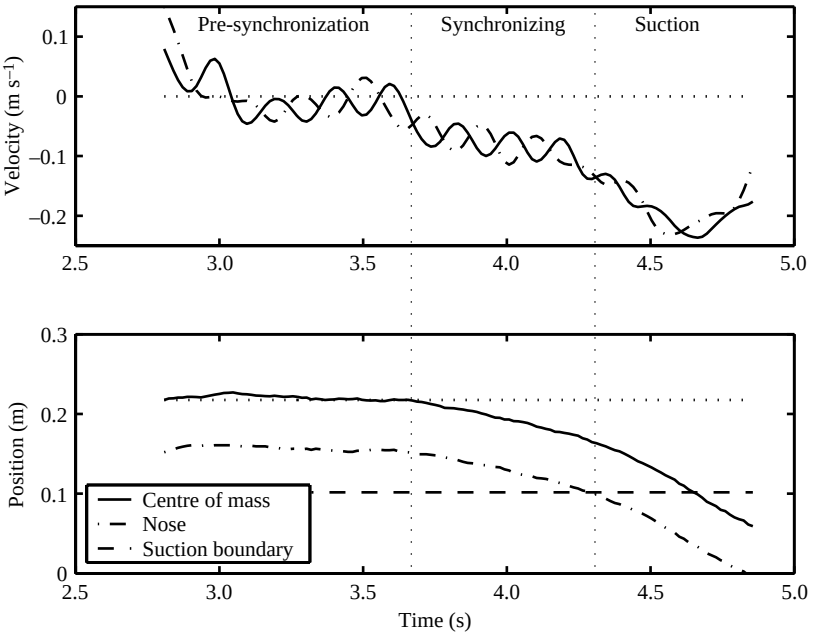

FIGURE 5. Downstream velocity and position of the centre-of-mass and nose of the dead trout. The cylinder back is located at position zero, and a negative velocity is upstream.

	Live trout	Dead trout
Mass (g)	19.5 ± 0.6	50.1
Length (cm)	12.9 ± 0.031	17.8
Head amplitude (D)	0.338 ± 0.015	0.239 ± 0.017
Centre of mass amplitude (D)	0.317 ± 0.017	0.184 ± 0.015
Mid-body amplitude (D)	0.340 ± 0.017	0.194 ± 0.018
Tail amplitude (D)	0.648 ± 0.025	0.484 ± 0.066
Relative frequency ω_f/ω_w	1.00 ± 0.01	1.01 ± 0.01
Relative wavelength λ_f/λ_w	1.94 ± 0.05	1.25 ± 0.06
Head angle amplitude (deg.)	5.4 ± 0.5	18.5 ± 1.3

TABLE 1. Comparisons between live fish from the PIV tests and the dead fish, where all amplitudes of motion are relative to the mid-line, and frequency and wavelength are normalized by the corresponding values for the cylinder wake.

run, the fish begins to move forward and flap in synchronization with the oncoming vortices. After this point in time, the line is not taut. However, the fish continues accelerating forward, despite there being no forces on it other than those from the fluid. Once the suction region is reached at 4.3 s, the oscillatory motion begins to fall apart as the fish is pulled into the suction region, towards the cylinder base. The axial oscillations seen in the figure are perturbations due to the lateral flapping motion, at a frequency twice that of the lateral oscillations, as each point of the body moves in a figure-of-eight motion (transverse oscillatory motion at frequency f plus axial oscillatory motion at frequency $2f$).

Table 1 compares the kinematics of the dead fish with that of the trout used in the PIV experiments in Liao *et al.* (2003*b*). In both cases, the frequencies were closely matched to that of the wake. A visual comparison for a single period of motion is

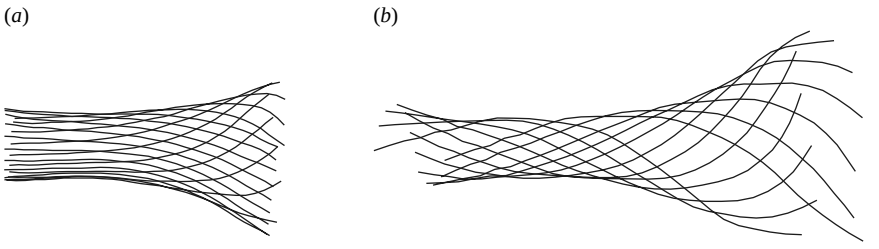

FIGURE 6. Trout mid-lines for a cycle of motion behind the cylinder wake for (*a*) a live trout and (*b*) a dead trout.

shown in figure 6. The amplitude of the dead fish motion is 58 % to 75 % of that of the live fish (centre-of-mass and tail, respectively), although it is uncertain whether this difference is caused by the fish being alive or dead, or just as a result of size and mass differences (since some time had passed between experiments and the trout had grown). Also, the dead trout's body-motion wavelength was equal to 1.25 times the wake wavelength, which is considerably shorter than that observed in the live trout, where it was 1.94 times the wake wavelength.

We found that the average head angle amplitude of oscillation for the dead fish was 3.4 times that of the live fish. Given that muscle activity near the head in live fish has been shown to synchronize with the cylinder wake (although not down the rest of the body; Liao *et al.* 2003*b*), it appears that live fish are stiffening their heads so as to avoid large-amplitude head motions. This may be for hydrodynamic reasons, or just to keep their view straight-ahead, instead of continually swinging the head from side-to-side.

3.3. *Discussion*

The only mechanism available for the dead fish to accelerate upstream against its own drag is the wake inducing the body to flap in such a manner as to generate thrust. As mentioned previously, Bose & Lien (1990) showed that whales are able to extract energy from the oscillating current across the whale's fluke generated by surface waves. As in our experiments, an oscillating flow is induced across the tail-foil – the body does not move in phase with the tail – which subsequently moves the entire body forward through the water. In one case, the flow is set up by surface waves; in the other, it is set up by a vortex street.

Considering the work by Liao *et al.* (2003*a*, *b*) in the light of dead fish results, a live fish must not only make certain that it stays within the wake, but also that is does not drift too far forward or backward. Essentially, the optimum position in the wake is an unstable one, such that if the fish drifts too far forward it will be sucked into the back of the cylinder, but if it drifts too far back it has to spend energy producing thrust. The preference of trout for positioning themselves in this equilibrium may explain the high-frequency small-amplitude corrective beats that are employed, as well as the considerable amount of pectoral-fin activity. Lending support to this interpretation, fish appear to improve their synchronization capability the longer they stay behind the cylinder.

4. Flapping foil

Having established a dead fish's capability to extract energy while producing net forward thrust through interaction with a vortex wake, we proceeded to test whether a mechanical device could produce a similar effect. We employed a

high-aspect-ratio foil placed behind a long D-cylinder in a cross-stream, an arrangement which has been used previously to establish vorticity control and energy extraction mechanisms (Gopalkrishnan *et al.* 1994; Anderson 1996). While earlier experiments had demonstrated energy extraction from the flow, they had never shown this energy to be sufficient for self-propulsion, although theoretical results had predicted it (Streitlien *et al.* 1996). In previous experiments, the foil was actively oscillated behind the cylinder and the effect of energy extraction was documented in terms of an increase in its propulsive efficiency. Instead, in the present experiments it was decided to allow the cylinder to oscillate in response to the oncoming excitation without external mechanical power – in analogy with the fish experiments – and measure both the energy in the system and the thrust on the foil.

The foil's performance was calculated through measurements of lift L, thrust T and pitch torque τ, in the form of the thrust coefficient C_T and power coefficient C_P, as defined below.

$$C_T = \frac{2\overline{T}}{\rho U^2 cs}, \qquad C_P = \frac{2\overline{P}_{in}}{\rho U^3 cs},$$

where c is the foil chord, s is the foil span, U is the towing speed, ρ is the density of water, and power input to the system from the motors is $P_{in}(t) = L(t)\dot{h}_f(t) + \tau(t)\dot{\theta}(t)$. Here, the foil's heave position is h_f, and its pitch position is θ. It should be noted that we measure thrust referenced to a zero obtained in still water, and hence the values reported represent the net forces produced by the foil, including thrust due to flapping and frictional drag effects.

First, experiments were run with a two-dimensional foil fixed in the wake of an oscillating cylinder, i.e. with the foil having no heave or pitch motion. These tests show that the foil does indeed produce thrust in the wake solely due to the effect of the undulating lateral flow across it (Katzmayr effect, e.g. Ober 1925), confirming that the thrust overcomes the foil's own drag, producing an excess thrust, with a $C_T = 0.030 \pm 0.006$ at $U = 0.4\,\mathrm{m\,s^{-1}}$. Although this demonstrates the passive production of net thrust within an oscillating wake, a better parallel to the fish studies described above was to show this net thrust production while the foil is allowed to oscillate passively within the unsteady wake, extracting energy as a power generator. The virtual damping of the oscillating foil apparatus represents the power-generating ability of the system, as it absorbs energy extracted from the foil's environment.

4.1. *Methods*

We tested a compliantly mounted, passive foil moving forward through an unsteady drag wake. The experiments make use of the foil and carriage apparatus described by Read, Hover & Triantafyllou (2003), with only a few changes. Following the same procedure as in Gopalkrishnan *et al.* (1994) and Anderson (1996), but unlike the tests with the fish, we oscillated the upstream D-section cylinder. An oscillating D-cylinder does not undergo a phase jump in vortex shedding as a function of the frequency, unlike circular cylinders; the vortices are always shed with the same phase angle relative to the motion for all frequencies. This allows the experimenter to have direct control on the phase of vortex-shedding and measure the relative phase between the foil motion and the vortices accurately – this makes the D-cylinders very suitable for such experiments. Comparing flow visualizations from Gopalkrishnan *et al.* (1994) and Anderson (1996), it was found that the form of the wake is similar to the wake in the fish experiments, with a regularly spaced array of two oppositely signed vortices per cycle shed from the upstream cylinder.

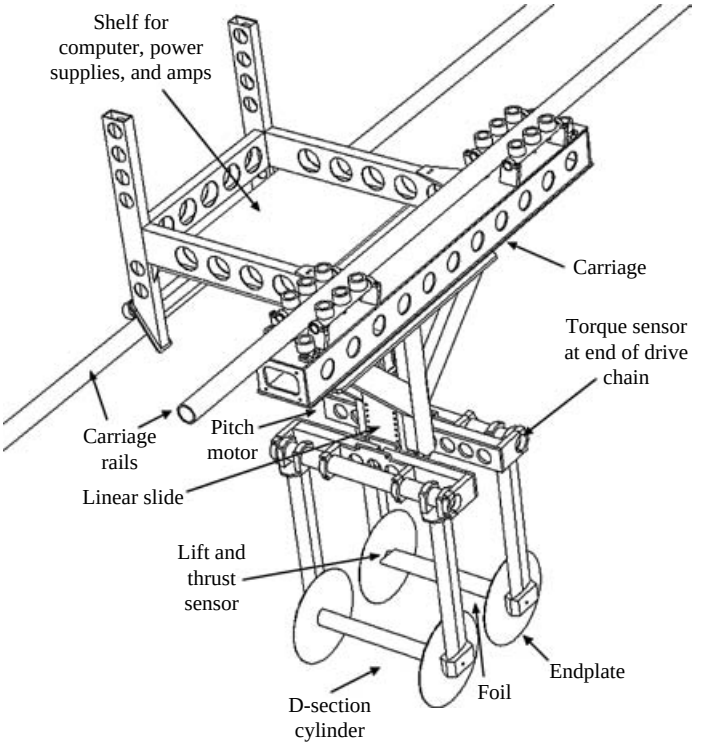

FIGURE 7. Diagram showing the foil and cylinder relative to the towtank carriage.

All of the mechanical hydrofoil experiments were performed at the MIT towing tank. The tank is 30 m long and 2.6 m wide, with a water depth of 1.14 m. A velocity-controlled testing carriage rests on a pair of rails which run down the length of the tank. A pair of lead-screws and linear tables are mounted to the carriage, in upstream and downstream positions, enabling computer-controlled motion in the vertical (heave) direction, as shown in figure 7.

The cylinder and rectangular foil are each mounted to the linear tables using vertical foil-shaped cross-section aluminium struts. Circular end-plates of 25 cm diameter are mounted to the aluminium struts at the ends of the foil and cylinder, in order to reduce three-dimensional effects. The 7.5 cm diameter, 60 cm span, polyethylene D-section cylinder is mounted onto the forward linear drive, and used as a vortex generator for the foil. The cylinder is set with a rearward-facing vertical flat face using a level. The distance from the connection point of the cylinder to the pivot of the foil is limited by the apparatus to $5D$, or $4.44D$ from the back edge of the cylinder to the leading edge of the foil. The cylinder and foil were zeroed to the same heave position using a level. The NACA 0012 cross-section foil is attached to the rear linear slide. It has a 60 cm span, 10 cm chord, and pitches around its quarter-chord point. One end of the foil is set into a load cell in order to measure the lift and thrust forces on the foil, while the other end is mounted to a chain and sprocket leading to a servomotor which controls the foil in pitch through a torque sensor. A potentiometer returns the absolute pitch position. Hence, the foil and cylinder heave positions, as well as the instantaneous lift, thrust, torque and pitch position for the foil were recorded. The load cells were calibrated using hanging weights. Kistler load cells have slight cross-talk between thrust and lift axes, so the cross-correlation terms were also calibrated. As the

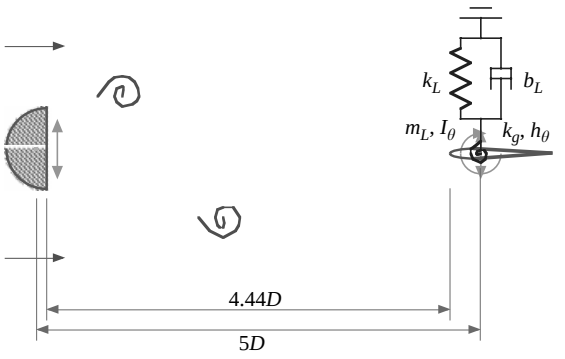

FIGURE 8. Through the use of force feedback, the foil is modelled as if supported by a spring–mass–damper in both heave and pitch.

forces measured in these experiments were relatively small compared to those by Read *et al.* (2003), the apparatus was calibrated with a minimum weight of 0.5 N as a test of the sensor resolution.

Virtual compliant mounting in heave and pitch was achieved via force-feedback. Using the measured forces on the load sensors, the control system calculated the resulting velocities induced on the foil in heave and pitch, through a spring–mass–damper model. Figure 8 illustrates the desired effect. The virtual systems for the heave and pitch motions are as follows:

$$L(t) = m_h\ddot{h}(t) + b_h\dot{h}(t) + k_h h(t),$$
$$\tau(t) = I_\theta\ddot{\theta}(t) + b_\theta\dot{\theta}(t) + k_\theta\theta(t),$$

where m_h, b_h and k_h are the mass, damping and stiffness of the heave virtual system, and I_θ, b_θ and k_θ are the rotational inertia, damping and stiffness in the pitch direction. These equations are coupled through the lift force and torque moment. For instance, moving in heave creates a torque about the foil pivot which induces motion in pitch, and vice versa.

In order to model best the virtual system presented above, the actual mass of the foil must be subtracted out and, since the pitch axis measures torque through the chain drive, the actual pitch damping and inertia should be subtracted out as well. The foil mass was measured ($m_{h,actual} = 0.277\,\mathrm{kg}$), and the rotary inertia and damping were measured by pitching the foil sinusoidally back-and-forth in air, at the desired frequency. The measured torque could then be broken down into components which are in-phase with the position (which must be compliance or inertia) and components which are 90° out-of-phase with the position (which must be damping). Through this method, the pitch inertia and damping were estimated as $I_{\theta,actual} = 0.000333\,\mathrm{kg\,m^2}$ and $b_{\theta,actual} = 0.00625\,\mathrm{kg\,m^2\,s^{-1}}$, respectively. Note that this value of $I_{\theta,actual}$ includes the effect of the centre-of-mass not being located at the foil pivot point. Additionally, the fact that the moment arm for the effects of gravity changes with pitch is not reflected in the above pitch equation is inconsequential, as the pitch angles measured in these experiments are small. The power values we calculated are, in any event, based on the measured force, torque and motions and are therefore transparent to the efficacy of the force feedback system to match the desired dynamics.

The state equations for heave and pitch were developed in MATLAB in continuous time, discretized using a bilinear approximation, and then solved for the transfer functions relating the velocities $\dot{h}$ and $\dot{\theta}$ to the inputs L and τ. The control loop

Heave	Pitch
$\omega_h = 13.193$ rad s^{-1}	$\omega_\theta = 13.193$ rad s^{-1}
$\zeta_h = 0.01$	$\zeta_\theta = 0.01$
$m_h = 14.71$ kg	$I_\theta = 0.0263$ kg m^2
$b_h = 3.88$ kg s^{-1}	$b_\theta = 0.0069$ kg m^2 s^{-1}
$k_h = 2560$ kg s^{-2}	$k_\theta = 4.5837$ kg m^2 s^{-2}

TABLE 2. Parameters used in the force-feedback experiments.

frequency was 250 Hz. The system reacted poorly to low virtual masses (of the order of the actual foil mass), exhibiting a high-frequency shaking that drowned out the forces in the experiments. This was due to small time lags and backlash in the control system, actuators and gearing, which prevented the system from reacting instantaneously and in the proper phase to force input. This is a fundamental problem in force feedback systems; by increasing the virtual mass, however, the chattering can be eliminated, so that the system exhibits smooth motion and reacts intuitively to manual pushing. Thus, the virtual system mass, stiffness and damping coefficients were chosen in order to meet a desired resonant frequency, with a mass low enough that the self-induced motion had time to develop during the run in the tank, yet high enough to avoid the chattering problems discussed above. We also needed a damping value low enough that the system could resonate with the input forcing at a reasonable amplitude. The virtual parameters used for the tests presented here are given in table 2.

We found that the forcing was stronger and the resulting foil amplitudes higher when the cylinder amplitude was also low. Additionally, energy in the wake and measured forces would be larger at a higher carriage velocity. Hence, all tests presented here used cylinder heave amplitude $H_c = 0.1D$, cylinder Strouhal number $St_c = 2H_c\omega/(2\pi U) = 0.04$, with a carriage velocity $U = 0.8$ m s^{-1} giving a Reynolds number based on cylinder diameter of 60 000. Results presented are averages of five tests.

4.2. *Results*

A typical case in shown in figure 9. The steady-state amplitudes and forces were low, relative to the tests performed by Read *et al.* (2003), reaching an average heave amplitude $h_f/D = 0.139 \pm 0.017$ and pitch amplitude $\theta_o = 0.107 \pm 0.021$ rad. The heave and pitch amplitudes were not necessarily steady over the course of the run, sometimes falling in amplitude before increasing again, but not in a way that would suggest a beating motion. We see that once the foil starts its passive motion, the lift forces decrease in magnitude and periodicity, because the angle of attack is reduced and modulated by the motion. In the limit, as the foil is moving with the fluid, the excitation lift force becomes nearly zero and a dynamic equilibrium is obtained.

The thrust and power recorded relatively low average values, positive and negative, respectively, but larger than the measurement uncertainty level by about an order of magnitude. The instantaneous thrust and energy were seen to occasionally switch sign, from negative and positive values, over a portion of a cycle. The mean thrust and power coefficients were $C_T = 0.017 \pm 0.004$ and $C_P = -0.0071 \pm 0.001$, corresponding to thrusts of 0.27 ± 0.06 N and a power of -0.090 ± 0.012 W. It should be noted that the drag coefficient of the foil, towed at zero heave and pitch motion in open flow, was measured to be $c_D = 0.028$ at Reynolds number $Re = 80\,000$ and

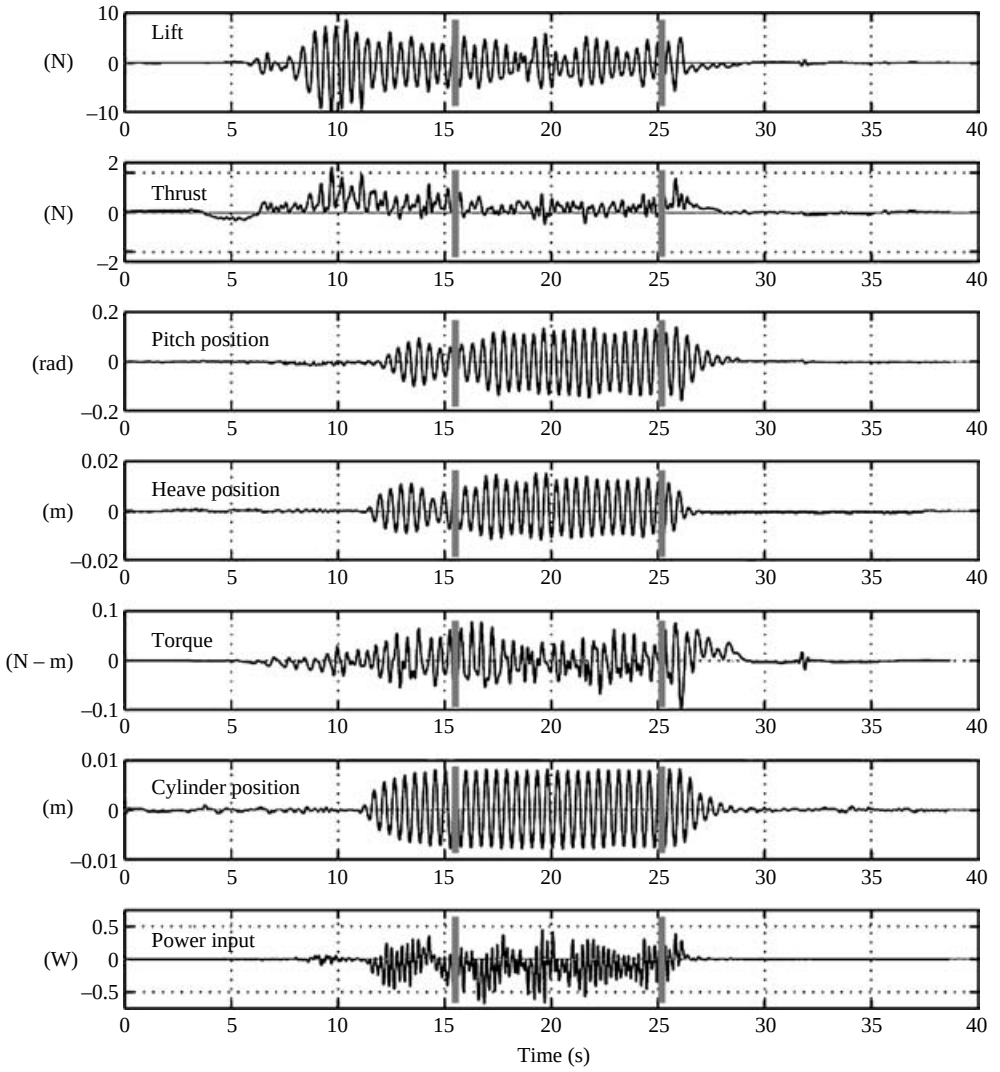

FIGURE 9. During this run, carriage motion was started at time $t = 4$ s. The cylinder heaving and force-feedback algorithms were started at $t = 11$ s and ended at 26 s. Data were collected between the vertical thick lines.

$C_D = 0.0652$ at $Re = 30\,000$. The drag coefficient increases only slightly when the foil is oscillating with small motions (Anderson *et al.* 1998), and hence an estimate of the hydrodynamically produced thrust coefficient is $C_{TH} = 0.067$, with an assumed drag coefficient of $C_D = 0.050$.

The average phase angle between foil and cylinder heave motion was $\phi = 323 \pm 7°$. Using the measured phase angle, the relative distance between foil and cylinder, and data from forced foil motion behind a cylinder (Gopalkrishnan *et al.* 1994; Beal 2003), we established that the foil operates, within $\pm 7°$ of phase, in a slaloming mode, i.e. a mode where the foil narrowly avoids intercepting the oncoming eddies, while the wake consists of pairs of vortices, one from the cylinder and one from the foil. In the experiments with live fish behind D-cylinders (Liao *et al.* 2003*b*) the same slaloming mode is found, establishing a close connection between the energy

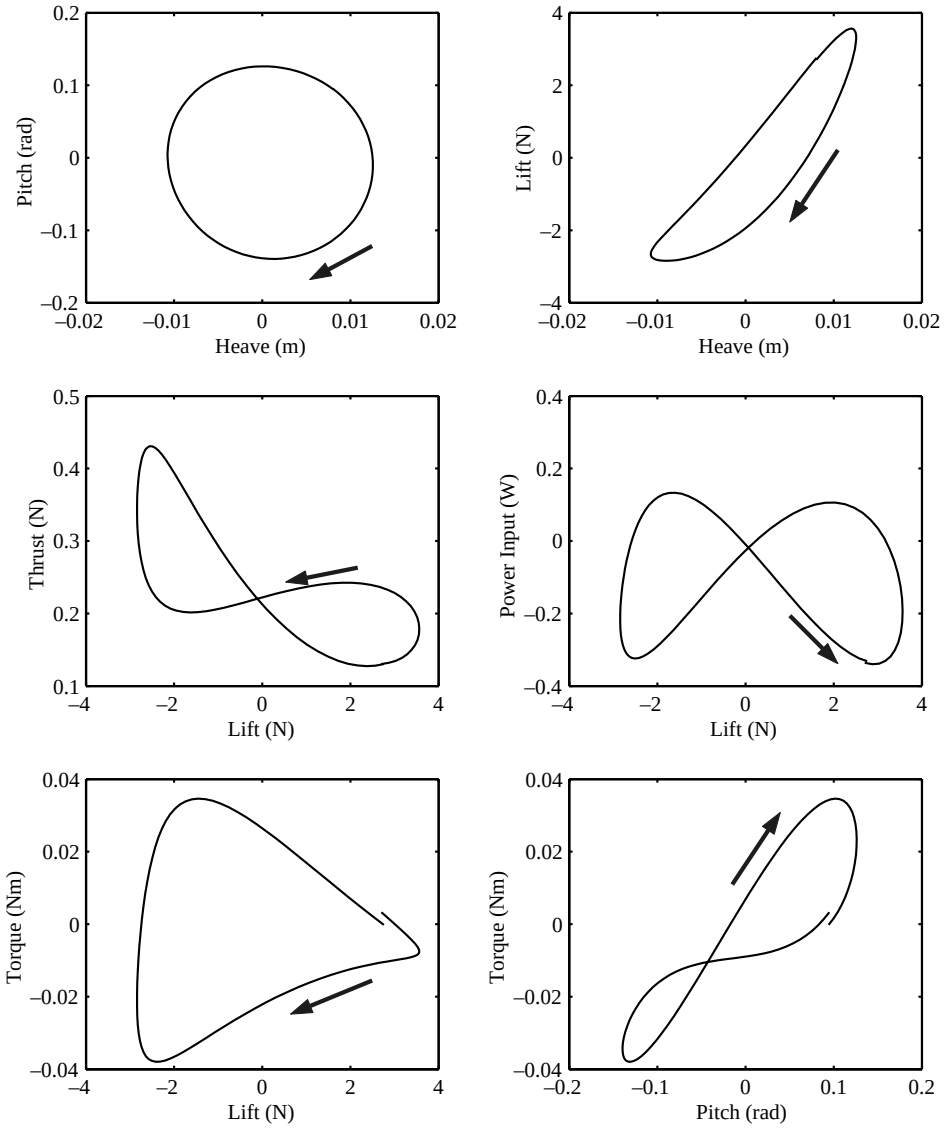

FIGURE 10. Comparison of phase-averaged signals for passive motion within the wake.

extraction mode employed in the two-dimensional foil and the mode employed by the three-dimensional fish.

The heave and pitch motions were approximately 90° out of phase, as seen in figure 10, which also compares several other output variables from the force-feedback runs. Lift and heave were not quite in phase, with the lift leading the heave position by $28.4° \pm 6.4°$; similarly, the torque led the pitch position by $31.4° \pm 5.6°$. We note that the runs performed by Read *et al.* (2003) revealed that the heave and pitch motions, for good performance in a driven foil in uniform flow, are also out of phase by 90°, and further that the lift force is nearly in phase with the heave velocity. The discrepancy on the latter comparison is explained by the presence of vortices in the flow. In the case of uniform inflow and driven motion, the lift force in phase with velocity shows nearly complete dissipation of mechanical power, with very little

added mass effect. In contrast, the vortical wake that excites the compliantly mounted foil does so with individual, convecting vortices, and a potentially larger added mass effect. It remains to be seen whether more careful tuning of the resonance could modify the behaviour of the passive foil.

As seen in figure 10, two thrust peaks were present, as also observed during forced-motion runs, but one thrust peak was significantly weaker than the other. The explanation is that at the relatively low forces and amplitudes involved, some asymmetry existed, owing to a combination of small errors in the levelling between the cylinder and the foil (giving a physical asymmetry in the flow relative to the foil), an error in precisely zeroing the pitch axis, small errors in the cross-terms of the calibration, and small differences in the mechanical foil heave actuation in upwards versus downwards directions, working with or against gravity. Despite this asymmetry, mean thrust production with mean power extraction is clearly demonstrated. Indeed, the forces at the beginning and end of the trial were measured to be zero, whereas the mean thrust is non-zero and positive in between, with a negative calculated power, showing thrust production with energy extraction.

4.3. *Discussion*

Overall, there are two mechanisms at work. First, there is a lift and thrust producing mechanism, related to the work by Wu (1972) for water waves, where the relative angle of attack induced by the lateral flow is the principal parameter. Within this mechanism, forces become larger if the foil moves against the lateral flow. For the flexing fish, this is easier to achieve than for a rigid foil. When the fish oscillates in its first natural flexing mode, for example, the tail, which produces most of the thrust, moves in antiphase with respect to the head. If the length of the fish is comparable to the wavelength of the flow, then the excitation force along the length has considerable phase variation to allow the tail to move out of phase with respect to the local flow. For this reason the tail of the fish can generate enough excess thrust to overcome the drag over the entire body.

A second mechanism for thrust production is the suction caused by the oncoming large-scale eddies, although it is not separable from the first mechanism, because the eddies are embedded in the flow. This vortex–foil interaction is an additional effect, not accounted for in Wu's work, which depends principally on the timing between the arrival of the vortices at the leading edge of the foil and the relative lateral position of the foil. The wake of a cylinder is characterized by the regular large-amplitude eddies of the Kármán street, and their interactions with the foil are in accordance with the principal mechanisms studied by Gopalkrishnan *et al.* (1994), Anderson (1996) and Beal (2003), which can enhance or decrease thrust and efficiency. The studies of Gopalkrishnan *et al.*, Anderson and Beal were for a large-aspect-ratio foil, whose vortices were comparable in aspect ratio to the Kármán street vortices, similarly to the passive foil studied here. For the fish, its tail span is only a fraction of the upstream cylinder span (less than 10 %), and its shed vorticity is clearly three-dimensional within the nominally two-dimensional cylinder wake; hence, the Kármán vortices cannot be repositioned by the tail, they can just be distorted locally, over a distance equal to the foil span. As a result, a vortex pairing is the most likely mode, equivalent to the 'slaloming mode' of Streitlien *et al.* (1996), because within this mode, the foil sheds vortices close to the cylinder vortices to pair up with them, but does not reposition them. It so happens, however, that this is a high-efficiency mode, and hence it is employed by both the live fish with the three-dimensional body, as established by Liao *et al.* (2003*b*) through PIV, and by the very high-aspect-ratio mechanical foil.

In terms of the amount of energy extraction, the result is even more impressive for the mechanical foil than for the fish, because it recovers energy over a large span, comparable to the cylinder span.

In summary, the three-dimensional tail of the fish within a two-dimensional wake and the two-dimensional foil within a wake follow a similar basic principle of vorticity control to extract energy from the flow. What is remarkable is that, in both cases, the net thrust exceeds drag, providing for perpetual tracking by the downstream object.

5. Conclusions

We show conclusively that a streamlined body passively oscillating within a vortical wake can extract sufficient energy from the turbulent eddies to propel itself upstream. This mechanism allows a body – under the proper conditions – to indefinitely track another body which generates this vortical wake. It also points toward novel low-drag energy harvesting devices, operating in air and in water.

In the case of the dead fish, energy extraction is achieved when the flexible body resonates in a natural mode with oncoming Kármán street eddies, generating sufficient thrust to overcome its own drag. This is in agreement with the live rainbow trout tests by Liao *et al.* (2003*a*, *b*); the fish are not just positioning themselves behind the cylinder in order to draft within the velocity deficit, but are also extracting energy from the vorticity.

In the case of the passively mounted high-aspect-ratio foil, positive axial force is generated at negative power, i.e. the foil extracts energy and simultaneously generates sufficient thrust to overcome its drag. In this case, owing to the large foil span, energy extraction is far more extensive than in the case of the small-span fish, making the result important for applications.

The authors wish to acknowledge support from the MIT Sea Grant Program under grant NA46RG0434, and from ONR under grant N00014-95-1-1106 for the development of the virtual flexible apparatus.

REFERENCES

Allen, J. J. & Smits, J. 2001 Energy harvesting eel. *J. Fluids Struct.* **15**, 629–640.

Anderson, J. M. 1996 Vorticity control for efficient propulsion. PhD thesis, Massachusetts Institute of Technology, Cambridge, MA.

Anderson, J. M., Streitlien, K., Barrett, D. S. & Triantafyllou, M. S. 1998 Oscillating foils of high propulsive efficiency. *J. Fluid Mech.* **360**, 41–72.

Beal, D. N. 2003 Propulsion through wake synchronization using a flapping foil. PhD thesis, Massachusetts Institute of Technology, Cambridge, MA.

Bose, N. & Lien, J. 1990 Energy absorption from ocean waves: a free ride for cetaceans. *Proc. R. Soc. Lond.* **240**, 591–605.

Braun, C. B. & Coombs, S. 2000 The overlapping roles of the inner ear and lateral line: the active space of dipole source detection. *Proc. R. Soc. Lond.* B **355**, 1115–1119.

Drucker, E. G. & Lauder, G. V. 2001 Locomotor function of the dorsal fin in teleost fishes: experimental analysis of wake forces in sunfish. *J. Exp. Biol.* **204**, 2943–2958.

Fausch, K. D. 1984 Profitable stream positions for salmonids: relating specific growth rate to net energy gain. *Can. J. Zool.* **62**, 441–451.

Fejer, A. A. 1960 Porpoises and the bow-riding of ships under way. *Nature* **188**, 700–703.

Fish, F. E. 1999 Energetics of swimming and flying in formation. *Comments Theor. Biol.* **5**, 283–304.

Gerrard, J. H. 1966 Formation region of vortices behind bluff bodies. *J. Fluid Mech.* **25**, 401–413.

Gopalkrishnan, R., Triantafyllou, M. S., Triantafyllou, G. S. & Barrett, D. 1994 Active vorticity control in a shear flow using a flapping foil. *J. Fluid Mech.* **274**, 1–21.

Isshiki, H. & Murakami, M. 1984 A theory of wave devouring propulsion (4th Report). *J. Soc. Naval Architects Japan* **156**, 102–114.

Koochesfahani, M. M. & Dimotakis, P. E. 1988 A cancellation experiment in a forced turbulent shear layer. *AIAA J.* **88**, 3713.

Liao, J. C., Beal, D. N., Lauder, G. V. & Triantafyllou, M. S. 2003*a* The Kármán gait: novel body kinematics of rainbow trout swimming in a vortex street. *J. Exp. Biol.* **206**, 1059–1073.

Liao, J. C., Beal, D. N., Lauder, G. V. & Triantafyllou, M. S. 2003*b* Fish exploiting vortices decrease muscle activity. *Science* **302**, 1566–1569.

Mueller, U. K., van der Heuvel, B.-L. E., Stamhuis, E. J. & Videler, J. J. 1997 Fish foot prints: morphology and energetics of the wake behind a continuously swimming mullet (*Chelon labrosus risso*). *J. Exp. Biol.* **200**, 2893–2906.

Mueller, U. K., Smit, J., Stamhuis, E. J. & Videler, J. J. 2001 How the body contributes to the wake in undulatory fish swimming: flow fields of a swimming eel (*Anguilla anguilla*). *J. Exp. Biol.* **204**, 2751–2762.

Ober, S. 1925 Note on the Katzmayr effect on airfoil drag. *NACA TN* 214.

Read, D. A., Hover, F. S. & Triantafyllou, M. S. 2003 Forces on oscillating foils for propulsion and maneuvering. *J. Fluids Struct.* **17**, 163–183.

So, R. M. C., Jadic, I. & Mignolet, M. P. 1999 Fluid-structure resonance produced by oncoming alternating vortices. *J. Fluids Struct.* **13**, 519–548.

Streitlien, K., Triantafyllou, G. S. & Triantafyllou, M. S. 1996 Efficient foil propulsion through vortex control. *AIAA J.* **34**, 2315–2319.

Sutterlin, A. M. & Waddy, S. 1975 Possible role of the posterior lateral line in obstacle entrainment by brook trout. *J. Fisheries Res. Board Can.* **32**, 2441–2446.

Tytell, E. D. & Lauder, G. V. 2004 The hydrodynamics of eel swimming: I. Wake structure. *J. Exp. Biol.* **207**, 1825–1841.

Videler, J. J. 1993 *Fish Swimming*. Chapman & Hall.

Wolfgang, M. J., Anderson, J. M., Grosenbaugh, M. A., Yue, D. K.-P. & Triantafyllou, M. S. 1999 Near-body flow dynamics in swimming fish. *J. Exp. Biol.* **202**, 2303–2327.

Wu, T. Y. 1972 Extraction of flow energy by a wing oscillating in waves. *J. Ship Res.* March, 66–78.

Wu, T. Y. & Chwang, A. T. 1974 Extraction of flow energy by fish and birds in a wavy stream. *Proc. Symp. on Swimming and Flying in Nature* (ed. T. Y. T. Wu, C. J. Brokaw & C. Brennan), pp. 687–702.